



# The Early Cretaceous Transition from Carbonate to Siliciclastic Deposition in the Deep Waters of the Northern Gulf of Mexico: New Insights from the Keathley Canyon 102 #1 Well

Michael L. Sweet<sup>1</sup>, Marcie Purkey Phillips<sup>1</sup>, Robert Cunningham<sup>1</sup>,  
John W. Snedden<sup>1</sup>, and Ryan Weber<sup>2</sup>

<sup>1</sup>*Gulf Basin Depositional Synthesis Project, Institute for Geophysics,  
The University of Texas at Austin, Austin, Texas 78758, U.S.A.*

<sup>2</sup>*Paleodata Inc., 6619 Fleur de Lis Dr., New Orleans, Louisiana 70124, U.S.A.*

## ABSTRACT

The Early Cretaceous in the northern Gulf of Mexico was a time of widespread carbonate deposition. The catchment area of clastic sediment directed into the Gulf of Mexico was relatively small. Moreover, a rimming carbonate margin prevented the movement of any significant volume of siliciclastic sediment, especially sand, into deep water. This depositional system changed dramatically, but briefly, in the Albian and Cenomanian with a shift to siliciclastic deposition recorded by the Tuscaloosa Group. The latest Cretaceous marked a return to carbonate deposition in the Navarro-Taylor supersequence up to the time of the Chicxulub Impact.

In this paper, we investigate a phase of clastic deep-water deposition during the Cretaceous with a new biostratigraphic age model integrated with core sedimentology and well log correlation, for the deep-water siliciclastic rocks encountered in the Keathley Canyon (KC) 102 #1 (Tiber) well. These data suggest that the transition to siliciclastic deposition in deep water began in the Albian, earlier than previously thought. Our new age model shows that a large part of the 1650 ft thick section of deep-water siliciclastic rocks encountered in the Tiber well are Albian and associated with the Paluxy-Washita (PW) supersequence, not Cenomanian-Turonian Eagle Ford-Tuscaloosa (EFT) supersequence as previously thought. Furthermore, the sandstones seen in core from the PW and EFT supersequences are relatively coarse-grained as compared to other Cenozoic reservoirs ranging from fine sand to coarse sand and granules. A thick section of deep-water sandstone in this grain size range hundreds of miles from the contemporaneous shoreline suggests a direct connection between updip fluvial deltaic systems and submarine canyons routing sand into submarine fans.

Geochemical data identifies organically enriched shales above the sand-rich siliciclastic interval seen in the KC 102 #1 well, which we interpret as evidence for the Coniacian-Santonian Oceanic Anoxic Event (OAE) 3.

The occurrence of thick, sand-rich, deep-water deposits in the Albian is important for two reasons. First, it has significant implications for unraveling the paleogeography of North America in the Cretaceous, especially the orientation of fluvial drainage systems that fed these submarine fans. Secondly, Cretaceous deep-water reservoirs are an emerging play in the central Gulf of Mexico, as demonstrated in recent drilling campaigns. Understanding reservoir distribution is key to the success of this new play. Moreover, potential source rocks in the Cenomanian and Coniacian overlie these reservoirs in an optimal position to both charge and seal reservoir sandstone.

---

## INTRODUCTION

The Cretaceous stratigraphy of the Gulf of Mexico is complex, with a plethora of local formation and lithostratigraphic names. A number of these units occur entirely in the subsurface (e.g., the Norphlet Sandstone [Mancini et al., 1985]). For the purposes of this paper, we use the basin-wide supersequences defined by Snedden and Galloway (2019) based on micropaleontology, well log, and 2D seismic correlation. Of particular inter-

Geochronology			Stratigraphic Units by Area				GBDS Super-Sequences
Period	Epoch	Age	Western Gulf Coast	Central Gulf Coast		Eastern Gulf Coast	
Cretaceous	Late	Campanian	Taylor Group	Taylor Group		Selma Group	NT
			Brownstone Marl	Austin Gp.	Brownstone Marl		
		Santonian	Austin Gp.		Tokio Fm.	Eutaw Fm.	AC
		Coniacian					
		Turonian	Eagle Ford Gp.	Eagle Ford Gp.		Tuscaloosa Gp.	EFT
			Woodbine Gp.	Tuscaloosa Fm.			
	Cenomanian						
	Early	Albian	Washita Gp.	Washita Gp.	Washita Gp.	Dantzler Fm.	PW
			Fredericksburg Gp.	Goodland Limestone	Andrew Fm.	Fredericksburg Gp.	
			Paluxy Fm.	Paluxy Fm.	Paluxy Fm.	Paluxy Fm.	

Figure 1. Stratigraphy of the onshore and offshore Cretaceous in the Gulf of Mexico based on Swanson et al. (2013). In the right column are the supersequences of Snedden and Galloway (2019). NT = Navarro-Taylor, AC = Austin Chalk, EFT = Eagle Ford-Tuscaloosa, and PW = Paluxy-Washita.

est in this paper are the Paluxy-Washita (PW) and Eagle Ford-Tuscaloosa (EFT) supersequences (Fig. 1). Within these supersequences are a series of lithostratigraphic units such as the Albian Paluxy Formation and Dantzler Formation. This Upper Albian supersequence and the overlying Cenomanian/Turonian Tuscaloosa Group can be uniquely differentiated based on biostratigraphy.

In the northern Gulf of Mexico, the Albian was a time of largely carbonate deposition with broad carbonate platforms rimming the basin and restricting the movement of siliciclastic sediments into deep water (Salvador, 1991; Phelps et al., 2014; Snedden and Galloway, 2019). This depositional framework changed in the Cenomanian with the influx of siliciclastic rocks associated with the Woodbine and Tuscaloosa formations (Salvador, 1991; Snedden and Galloway, 2019; Snedden et al., 2022). Although the fluvial and deltaic facies of the Woodbine and Tuscaloosa are well known from outcrops and subsurface data, there are few penetrations of their coeval deep-water facies. Recent sediment volume mapping by Snedden et al. (2022) shows that significant volumes of sediment were deposited in the fluvial deltaic systems of the Albian PW supersequence in present-day southern Alabama, Mississippi, Georgia and the Florida Panhandle. Their mapping shows very limited sand bypass off the shelf, with major accommodation in a series of siliciclastic subsurface depocenters. In contrast, mapping suggests significant deep-water sedimentation linked to updip Cenomanian Tuscaloosa deltas and incised valleys (Wolf, 2012).

The objective of this paper is to describe the Cretaceous deep-water facies seen in newly released data from the Keathley Canyon (KC) 102 #1 Tiber well, determine their age, place them in a regional context, and discuss their significance for exploration in the Gulf of Mexico.

BP and partners drilled the KC 102 #1 well in 2009 to a depth of 35051 ft measured depth (MD) (Figs. 2 and 3). At the time, it was the deepest well drilled in the Gulf of Mexico. It is one of a small number of wells to encounter Cretaceous deep-water deposits in the northern Gulf of Mexico. Core photos from this well are the only publically released data on deep-water lithofacies from the Cretaceous interval in this area of the northern Gulf of Mexico. In addition to the KC 102 #1 well, several updip wells penetrate the Cretaceous; these helped us to understand slope channel-fill and deltaic deposits that record the feeder

systems to the submarine fans seen in KC 102 #1 (Fig. 4). Core and well log data indicate that these deep-water sandstones are not only over 1500 ft thick, they are relatively coarse grained with mean grain-size in the fine upper to medium lower sand size range and maximum grain sizes of coarse sand and granules.

Since the drilling of the KC 102 #1 well there have been no other tests of the Cretaceous deep-water play in the KC protraction area. Instead, the focus of exploration for this play shifted eastward to the Mississippi Canyon (MC) protraction area where two exploration wells have recently been drilled into the Mesozoic section—the BP Galapagos Deep prospect (MC 518 #2) in 2020, and in 2021 the Chevron MC 35 #2 Silverbank prospect (Fig. 2). Results of these wells are not publically available as of December 2022.

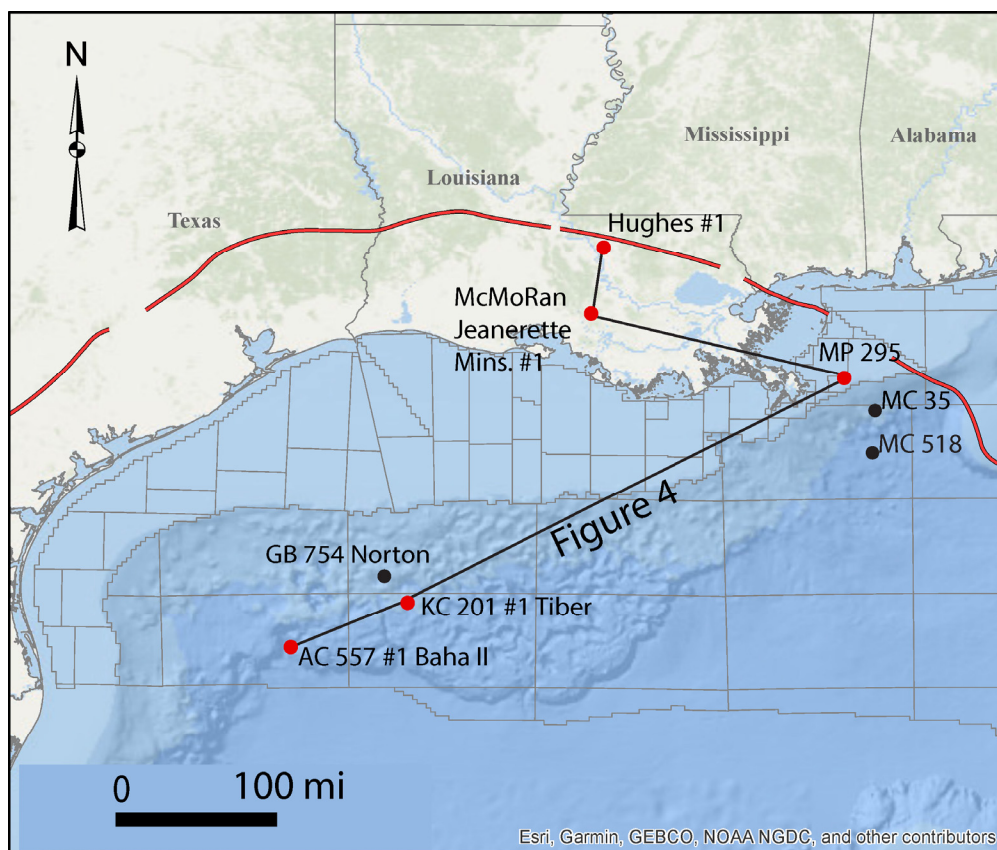
## DATA AND METHODS

### Biostratigraphy

We conducted an in-depth biostratigraphic re-interpretation of a 2000 ft interval through the Cretaceous section in the KC 102 #1 well using the publicly available raw biostratigraphy data initially collected by BP and onsite paleontologist (Digital Plate 1; see Appendix). Biostratigraphy data were collected from ditch cuttings at 30 ft intervals, a standard industry procedure.

Our first iteration of data interpretation applied traditional, industry-standard methods of identifying biohorizons—typically extinction events—of established marker species and applying their age datum (Waterman et al., 2017). Last appearance datums (LADs) and first appearance datums (FADs) of calcareous nannofossil and foraminifer marker species were recognized according to the widely applied Cretaceous and Upper Jurassic biostratigraphic chart of the Gulf Basin (Lu et al., 2019). We used the geologic time scale of Ogg et al. (2016) to ensure the most current stratigraphic calibrations. Two academic biozonations were also referenced: the classic nannofossil biozonation from Perch-Nielsen (1985); and Corbett et al. (2014) who produced a quantitatively-derived optimum sequence of nannofossil biostratigraphic events from the late Cenomanian to Coniacian using ranking and scaling (RASC) statistical analysis including datums with absolute ages. Our next approach applied FADs and/or LADs of non-marker species and genera, which yielded

**Figure 2.** Map of the Gulf of Mexico showing the location of the wells referenced in this paper. Red line shows the Albian shelf edge from [Snedden and Galloway \(2019\)](#). Wells MC 35 and MC 518 are reported to be recently drilled exploration wells testing the Cretaceous deep-water play in the eastern Gulf of Mexico.



enough useful age datum to make a conservatively reliable and informative biostratigraphic interpretation with which we were able to effectively address the study's objectives.

We produced distribution charts and interpreted them in conjunction with the biostratigraphy chart ([Digital Plate 1](#)). In contrast to biostratigraphic charts, which focus on select species intended for age interpretation, distribution charts plot all species, in order of observation from the top to the bottom of the hole, identified in each group of calcareous nannofossils and foraminifers, including total microfossil abundance curves. Distribution charts, therefore, are valuable tools for visualizing any abnormalities in microfossil distribution that may occur because of significant geological events and environmental shifts—abnormalities that may go unnoticed when applying only a regional stratigraphic datum chart.

Gamma ray and resistivity well logs were integrated with the biostratigraphy and incorporated on to the biostratigraphy chart to further constrain geologic age and interpret geological events recorded in KC 102 #1 ([Digital Plate 1](#)). Answers sought from biostratigraphy include identification of the Cenomanian/Turonian boundary, the oceanic anoxic events (OAEs), position of any major unconformities, interpreting the age of the sandstones previously interpreted as Tuscaloosa (Upper Cretaceous), and, finally, to interpret the geologic age at the base of hole (BOH).

### Core Data

BP released core photos, thin-section photos, porosity and permeability data, and petrophysical logs from the Cretaceous section in the KC 102 #1 well. We downloaded these data from the Bureau of Ocean Energy Management (BOEM) website (<https://www.data.boem.gov/>) for interpretation. Of particular interest were high-resolution core photos, thin-section photos, and porosity and permeability data from 235 ft of conventional

core taken in what we interpret as the Tuscaloosa Group, part of the EFT supersequence and the Dantzer sandstones of the Albian PW supersequence ([Fig. 3](#)). The well penetrated but did not core the Paluxy Sandstone. High quality core photos were used to describe lithology and sedimentary structures seen in core. Thin-section photos, that had a scale in mm, were used to measure grain size. We did not gather or have access to petrographic data on framework mineralogy. We did not have access to the core to sample it for other data such as detrital zircon analysis.

### Petrophysical Logs and Seismic Data

We used gamma ray and resistivity logs to infer lithofacies (sandstone, mudstone, and limestone). Log motifs (e.g., cleaning-up, fining-up) gave clues to environment of deposition. Given the burial depth of over 30,000 ft below the seafloor, available 2D seismic reflection data were not useful for determining depositional environment.

### Geochemical Data

Bulk geochemical data, total organic carbon (TOC, in weight % organic carbon) and Rock-Eval hydrogen index values (HI, in mg hydrocarbon HC/g TOC) were taken from previous geochemical studies on three industry wells (Garden Banks [GB] 754 #1 Norton, Alaminos Canyon [AC] 557 #1 Baha II, and KC 102 #1 Tiber) retrieved from the Bureau of Safety and Environmental Enforcement (BSEE) data repository (<https://www.data.bsee.gov/>) ([Fig. 2](#)). The data were derived from sample-based measurements obtained mainly from ditch-cuttings samples at 30 ft to 60 ft intervals and secondarily from rotary sidewall cores. Stratigraphic relationships between organic-rich beds in the wells are demonstrated through correlation of biostratigraphic tops obtained from this study and the BSEE reports ([Fig. 5](#)). Additional aids for recognizing OAEs such as

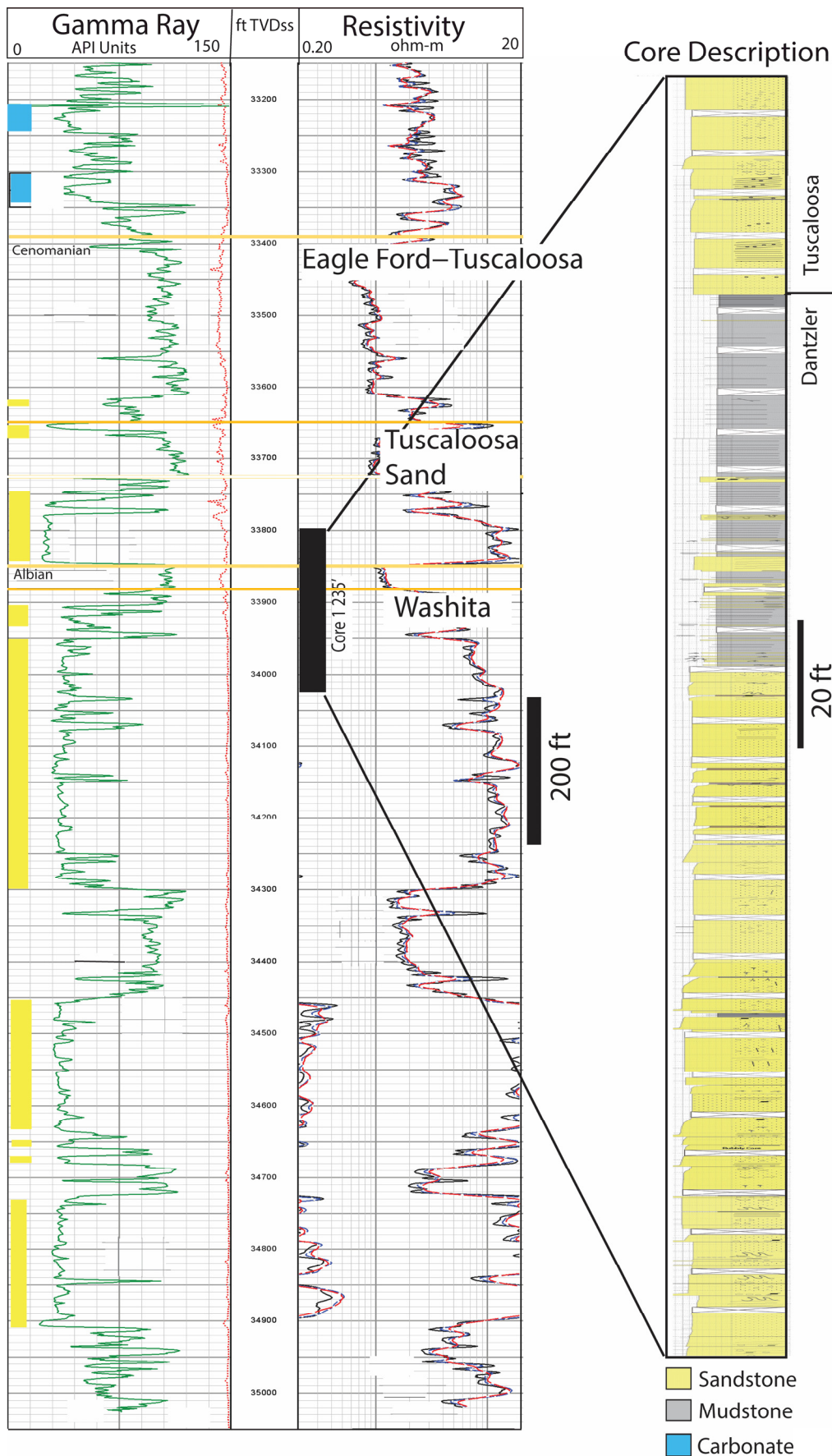
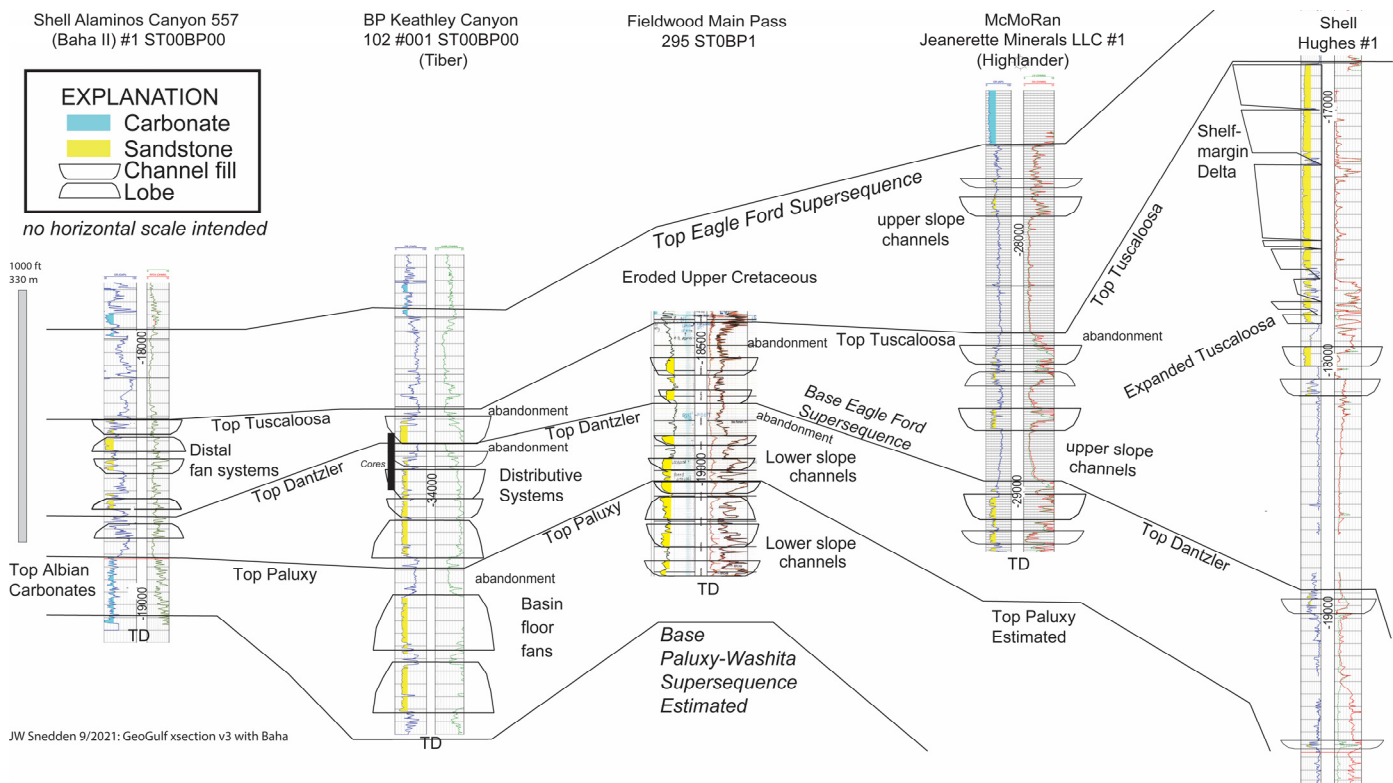


Figure 3. Wells logs showing the Cretaceous section in the KC 102 #1 well (left) and sedimentologic graphic log of the KC 102 #1 core (right).



**Figure 4.** Shelf to basin cross-section showing the stratigraphy and interpreted paleoenvironments of the Albian through Cenomanian-Turonian section in the northern Gulf of Mexico. The location of this cross-section is shown in Figure 2. Log motifs as shown in the legend are further explained in the text. Vertical scale on left. Equal spacing for wells used and location of wells shown in Figure 2.

carbon isotope stratigraphy were not available for this study, so assignments of organic-rich beds to individual OAEs are based on biostratigraphic ages and are considered provisional.

## RESULTS

### Geologic Age and Major Geological Events

We focused our re-interpretation of the biostratigraphy on the Cretaceous section of the KC 102 #1 well from 32,330 ft to 35,000 ft MD (Digital Plate 1). We interpret the Cretaceous/Paleogene boundary event at 32,330 ft MD, with associated impact related processes (cf Sanford et al., 2016) having truncated the section down to the lower Maastrichtian, according to the original biostratigraphy report (Bergen, 2009). The top Campanian is interpreted to be within the sample from 32,415–32,430 ft MD (Bergen, 2009).

From 32,430–33,390 ft MD the geologic age is interpreted to be Coniacian through Campanian (undifferentiated), and the Turonian is interpreted to be entirely truncated. Our interpretation is based primarily on the first occurrence (FO) of *Micula decussata* at 33,360 ft MD (FAD, 89.77 Ma; Turonian/Coniacian boundary) and the FO of *Micula concava* at 33,300 ft MD (FAD, ~88 Ma; mid-Coniacian). The co-existence of these two species means the geologic age cannot be younger than Coniacian. Our interpretation is consistent with the original biostratigraphy report that noted a major stratal discontinuity in the upper Coniacian from 33,350–33,360 ft MD (Bergen, 2009).

In addition to truncation of the Turonian, we also interpret the strata containing the Cenomanian-Turonian OAE 2 were completely eroded based on the absence and/or truncation of several critical marker species (Corbett et al., 2014). The absence of gamma ray and resistivity log signatures characterizing

OAE 2 (Lowery et al., 2017) and multiple major stratal discontinuities observed and noted in the original biostratigraphy report (Bergen, 2009) also point to a significant unconformity (Fig. 5).

The Cenomanian/Coniacian boundary, therefore, is interpreted at 33,390 ft MD, and is also interpreted to be truncated based on a significant uphole decrease in total microfossil abundance, a characteristic often indicative of a major geological event that disturbed the environment and the established ecosystem. Supporting our interpretation of this stage boundary are the last occurrences (LO) of calcareous nannofossils *Rhagodiscus asper* (LAD, 93.9 Ma) and *Corolithion kennedyi* (LAD, 94.64 Ma) at 33,390 ft MD. Supporting the interpretation of an unconformity is the observation of *Broinsonia signata* (LAD, 99.9 Ma) at 33,390 ft MD, although it is a single occurrence. The original biostratigraphy report noted another major stratal discontinuity in the upper Cenomanian from 33,390–33,420 ft MD (Bergen, 2009).

Just below the Cenomanian/Coniacian boundary, at 33,400 ft MD, we interpreted the top EFT supersequence based on log signatures. Within the Cenomanian, the top of the lower Tuscaloosa sand is interpreted at 33,650 ft MD.

The Cenomanian/Albian boundary, interpreted at 33,850 ft MD, is another disconformable surface. Supporting this interpretation is the occurrence of calcareous nannofossil *Braarudosphaera stenorhetha* (LAD, 100.49 Ma) (single occurrence). Further supporting this boundary interpretation and its likely truncation are the occurrences of foraminifers *Rotalipora appenninica* (LAD, 95.47 Ma), *Praeglobotruncana delrioensis* (LAD, 96.76 Ma), *Rotalipora subticinensis* (LAD, 102.42 Ma), and *Ticinnella roberti* (LAD, 101.48 Ma) that are all truncated at 33,850 ft MD. The ranges of *Rotalipora appenninica* and *Rotalipora subticinensis* do not overlap, however, so *Rotalipora subticinensis*

may be reworked. Similar to the Cenomanian/Coniacian boundary, there is also a significant shift in total microfossil abundance across this boundary indicating a significant geological event, and/or environmental shift. Integrated with the biohorizon, the well log signatures and lithostratigraphy align with and inform what we interpret as the base of a thick Tuscaloosa sand package.

From 33,850 ft MD to the bottom of the hole, the biostratigraphy-based geologic age is interpreted to be Albian. Although microfossils are sparse, several species with concomitant ranges through the Albian were observed including calcareous nannofossils *Watznaueria barnesae*, *Cretarhabdus conicus*, *Discorhabdus ignotus*, *Rhagodiscus angustus*, *Eiffelithus turris-eiffelii*, *Zeugrhabdotus embergeri*, *Tranolithus orionatus*, *Nannococcus regularis*, *Rhagodiscus achlyostaurion*, *Chiastozygus platurhethus*, *Prediscosphaera columnata*, *Braarudosphaera stenorhetha*, and *Nannococcus truitii*, along with foraminifers *Rotalipora appenninica* and *Rotalipora* spp. Several of these observed species also co-existed through the Aptian, but we do not interpret strata any older than Albian here based on the absence of *Hedbergella trocoidea*, a planktonic foraminifer that reliably marks the Glen Rose (lower Albian) across the Gulf of Mexico. Our age interpretation at BOH is consistent with the original biostratigraphy report (Bergen, 2009).

### Regional Stratigraphic Framework

Well logs from the limited number of wells that penetrated the Cretaceous interval in the central Gulf of Mexico were correlated using biostratigraphy and regional 2D seismic data (Figs. 4 and 5). The Baha II well encountered Cretaceous deep-water sandstones, but they were thinner and lower net to gross (NTG) than in the KC 102 #1 well. The thick Albian sandstones encountered in the KC 102 #1 correlate to deep-water marls and carbonate-rich zones in Baha II. We have access to a limited amount of data from these wells. Our only tool to interpret their environment of deposition is the gamma-ray log motifs of these widely spaced wells. We observed fining-upward trends, interpreted as channel-fill deposits and upward-coarsening patterns, interpreted as channel-mouth lobe deposits. Given the sparse data and the distance of these wells from the coeval shoreline we infer that these wells record deposition on a submarine fan. The marls seen in Baha II record deposition at the margins of the fan seen in the KC 102 #1 logs. Moving up depositional dip, the MP 295 well encountered interbedded sandstones and mudstones with dominant fining and thinning upward log motifs that we interpret as lower-slope, channel-fill deposits, based on their log motifs and regional stratigraphic context. We interpreted these slope channel-fill deposits within all three units - the Paluxy, Dantzler, and Tuscaloosa. The Highlander well did not penetrate the Paluxy section. It encountered what we interpret as middle to upper slope channel-fill deposits in the Tuscaloosa Group and Dantzler Formations, with relatively thick, blocky to slightly fining upward gamma ray log patterns. The Shell Hughes #1 encountered a thick Tuscaloosa section, with massively thick upward thickening patterns indicated deposition in expanded shelf-edge deltas. Barrell (1997) described similar shelf-edge deltaic and slope channels-fill deposits for the deep Tuscaloosa trend of Louisiana. The Shell Hughes #1 did not penetrate the Albian section.

### Core Facies

Core from the KC 102 #1 well encountered two thickly bedded successions of sandstones with an intervening 57 ft thick mudstone interval (Fig. 3). The lower 145 ft of core are composed of well-sorted, upper fine to lower medium grained, structureless sandstones ('Ta' following the Bouma classification) with lesser quantities of coarse-grained, poorly sorted sandstones

('S beds' of Lowe [1982]), and cross-bedded (Tt) or low-angle laminated sandstones (Tb). Ripple-laminations and contorted bedding occur, but are uncommon. Sandstones beds are typically amalgamated and fine upward, although some beds near the top of the interval are separated by thin mudstones. The most striking feature of these sandstones is their grain-size. Mean grain size is upper fine to lower medium sand. There is a significant component of coarse sand and granule-size quartz grains. Sand this coarse is unknown in the Paleogene and relatively uncommon in the Neogene deep-water deposits from the Gulf of Mexico (Snedden and Galloway 2019).

The mudstone interval consists of dark grey-black beds and light grey laminations. Although it is difficult to determine conclusively from core photos, the darker beds are interpreted as fine siltstone/claystone and the light grey laminations are interpreted as very fine sandstones / coarse siltstones. The most common sedimentary structure is parallel, planar lamination. Ripple laminations occur in the lower, more sandstone/siltstone-rich part of the core along with some contorted beds. There are some burrows. This interval overall shows a fining-up and thinning-up trend, with more numerous and thicker very fine sandstone and coarse siltstone beds near the base of the interval. Biostratigraphic data suggest that the top of the mudstone interval represents a major unconformity. Although it is a sharp contact in core (Fig. 6), it does not display features seen in other deep-water condensed sections like reddening, increases in carbonate content, or intense bioturbation (Boulestex et al., 2020). It is possible that these features were eroded before deposition of the overlying sandstone. It is likely that this fine-grained interval represents abandonments of the PW submarine fans as it doesn't display the stacking patterns and abundant ripple-laminated sandstones and siltstones seen, for example, in levee deposits or fan fringe deposits.

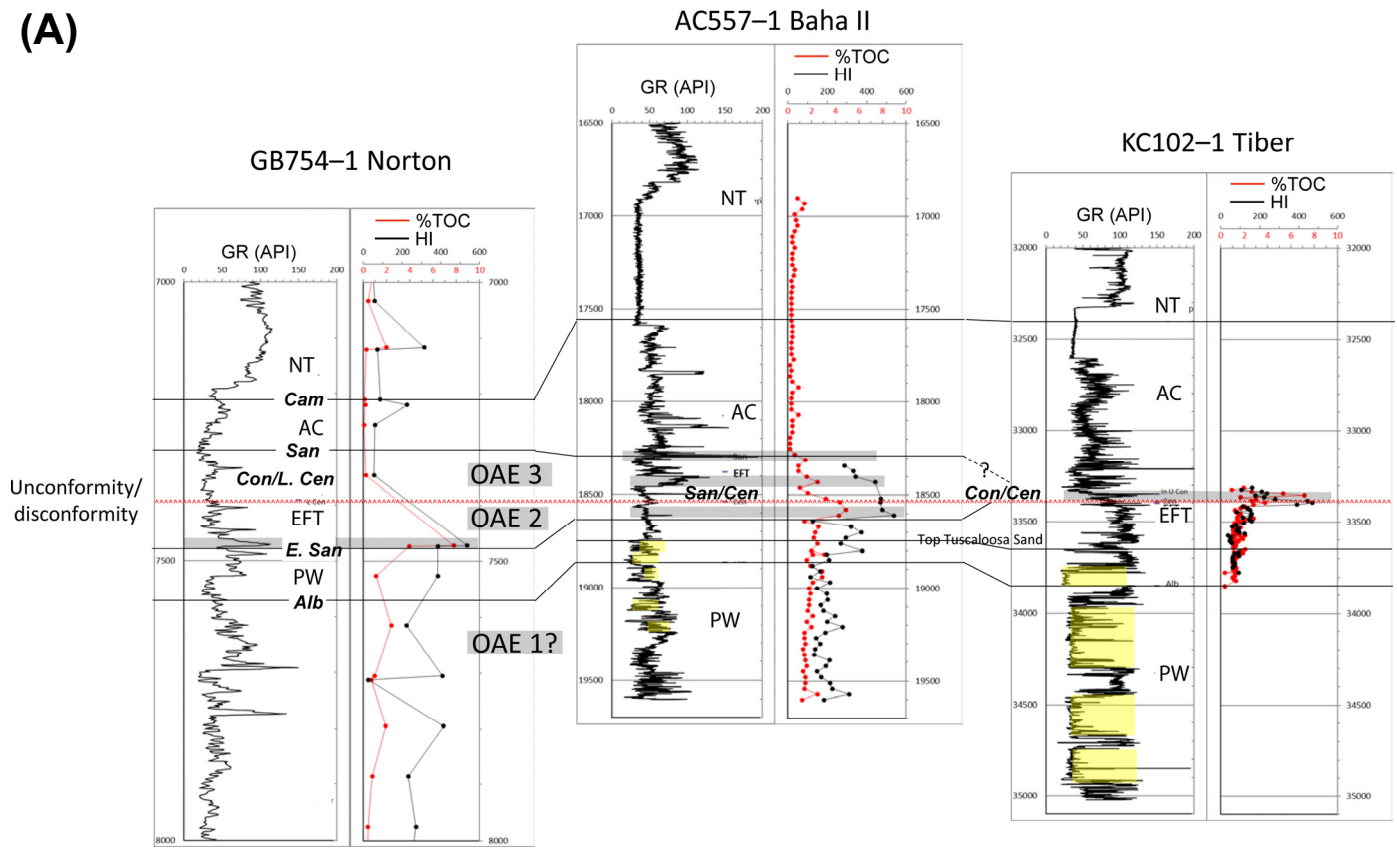
The upper most sandstone unit rests on a sharp contact with the underlying mudstone interval (Fig. 6). It is similar in terms of grain size (fine upper to medium lower) and sedimentary structures to the underlying sandstones. We did not evaluate their mineralogy to see if they share a common provenance.

The grain size and sedimentary structures seen in the Cretaceous sandstones are significantly different from the sandstones of the overlying Wilcox Group in two ways. First, they are significantly coarser grained than the Wilcox Group sandstones (fine upper to medium lower sand size versus very fine lower to fine lower sand size) and they have a component of medium upper to granule size grains that are not found in the deep-water Wilcox Group sandstones (Marchand et al., 2015). Second, muddy sandstones with organic matter commonly interpreted as hybrid flow or slurry deposits (e.g., Haughton et al., 2009) are rare. There could be two reasons for the dearth of slurry deposits. (1) The Cretaceous sandstones are coarser grained and lack the silt and organic content seen in deep-water deposits of the Wilcox Group that are characteristic of slurry deposits (e.g., Marchand et al., 2015). (2) The Cretaceous sandstones are generally well amalgamated with few interbedded mudstones, suggesting they were deposited in the updip and axial portions of submarine fan lobes where slurry deposits are uncommon. Slurry deposits usually occur on the lobe fringe (e.g., Haughton et al., 2009; Boulestex et al., 2020).

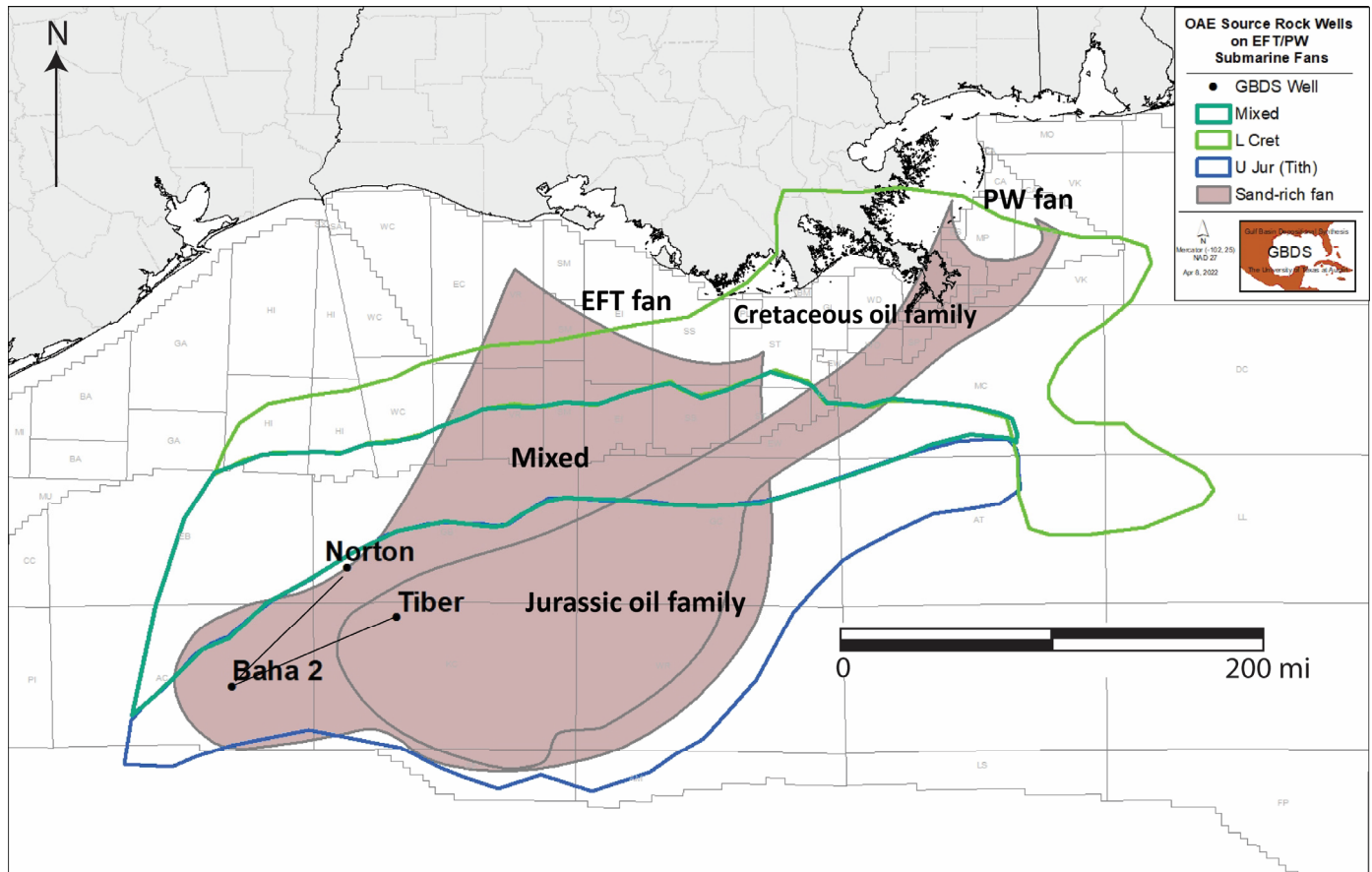
### Depositional Environments / Paleogeography

Core and petrophysical log facies, biostratigraphy, and depositional context indicate that the Cretaceous deep-water deposits in the KC 102 #1 well record two distinct deep-water depositional systems. The lower 775ft of blocky, thickly bedded sandstone belong to an Albian submarine fan deposited as much as 350 mi from the contemporaneous shelf edge (Fig. 7). Figure 7 shows a circuitous path for sediment moving from Albian deltas to the submarine fan seen in the KC 102 #1 well. This map is schemat-

(A)



(B)



**(FACING PAGE)** Figure 5. (A) Stratigraphic relationships of oceanic anoxic event (OAE) organic-rich source beds over PW and EFT submarine fans. Evidence for OAE 2 has been truncated at Tiber by the regional Cenomanian unconformity/disconformity. Potential OAE 1 organic enrichment is noted in the pre-Albian section at Norton and Baha II. Note vertical scale 3X expansion for Norton. Timelines (black) derived from biostratigraphic data are labelled: Cam = Campanian, San = Santonian, Con = Coniacian, Cen = Cenomanian, and Alb = Albian. The supersequences of [Snedden and Galloway \(2019\)](#) are labelled: NT = Navarro-Taylor, AC = Austin Chalk, EFT = Eagle Ford-Tuscaloosa, and PW = Paluxy-Washita. (B) Polygons of oil families, identified by source age, are superimposed on outlines of the EFT and PW submarine fans. Oil family polygons are after [Snedden et al. \(2020, their figure 9\)](#).

ic as we do not have enough well and seismic data to map in detail the connection between deltas and fans. Moreover, the geometry of the Albian margin is also not known in detail. Paleogeographic mapping by [Snedden et al. \(2016\)](#) and [Snedden and Galloway \(2019\)](#) shows that a carbonate shelf rimmed much of the northern Gulf of Mexico at this time. The only substantial deltaic system was fed primarily by the paleo-Apalachicola River and to a lesser extent, the paleo-Mississippi River ([Snedden et al., 2022](#)). Detrital zircon provenance data shows that these rivers largely drained the southern Appalachian Mountains ([Snedden et al., 2022](#)). Although no submarine canyons have yet been mapped in the Cretaceous of the northern Gulf of Mexico, the occurrence of thick, relatively coarse grained deep-water sandstones 100s of miles from the coeval shoreline suggests a long-lived connection between rivers, deltas and submarine fans ([Sweet and Blum, 2016](#)). Therefore, it is likely that fluvial/deltaic systems prograded across an early Albian carbonate platform and fed directly into submarine canyons at the shelf edge.

For reasons that are not clear at this time, sand delivered into the deep-water terminated in the Albian and submarine fans were abandoned for a time. When deep-water sand deposition resumed in the Cenomanian the primary source of sediment had moved westward to the paleo-Mississippi ([Fig. 9](#)) as documented in its subsurface depocenter ([Snedden et al., 2022](#)).

Although determining deep-water sub-environments from one well or core is fraught with uncertainty, the occurrence of relatively coarser grains, the high degree of sandstone bed amalgamation, higher net to gross and current-generated sedimentary structures, like cross-bedding and low-angle bedding, suggests that some of these sands were deposited in channels ranging from confined to distributive. Given the thick, blocky, and fining-up well log motifs ([Fig. 3](#)), vertical amalgamation, and location of these sandstones, we interpreted them to be the deposits of an extensive, basin-floor submarine fan that penetrated in the transition between feeder channels and lobes.

### Oceanic Anoxic Event Source Rocks

Hemipelagic sediments overlying the PW and EFT submarine fans contain lower Cenomanian to lower Campanian organic-rich, dark gray to black fine-grained marls and shales presumably related to the mid-Cretaceous Oceanic Anoxic Events (OAEs). The stratigraphic positions of these organic-rich beds are shown for Norton, Baha II, and Tiber ([Fig. 5](#)). TOC reaches 5–8% in the richest beds with HI exceeding 500 mg HC/g TOC, indicative of marine kerogen burial under oxygen deficient bottom waters. Organic-rich beds with age affinities closer to those of OAE 2, Cenomanian-Turonian, are observed in the Norton and Baha II wells, whereas those with ages occurring during OAE 3, Coniacian-Santonian, occur in Baha II and Tiber. Levels of TOC generally decline in the Albian and older sections in these wells, however values greater than 2% TOC and HI values above 300 mg HC/g TOC suggest Albian-Albian OAE 1 may have enhanced oxygen deficiency and organic carbon burial. High sedimentation rates in the submarine fan sequences may have diluted the organic supply or sampling bias may have limited the observation of greater organic enrichment. Although biostratigraphic and carbon isotopic constraints are lacking, these beds appear to

conform to the multiple discrete zones of organic-rich strata in OAEs 2 and 3 noted elsewhere in the Gulf of Mexico, Western Interior U.S., and globally ([Locklair et al., 2011](#); [Lowery et al., 2017](#)).

The unconformity capping the Cenomanian, recognized most notably in the KC 102 #1 well, may have eroded the OAE 2 organic-rich bed(s) there. The organic-rich bed lying above the Cenomanian unconformity in KC 102 #1 is likely in the lower Coniacian suggesting it may have been deposited during the latter stages of OAE 3. Erosion or non-deposition appears to have removed evidence of upper Cenomanian-Santonian organic enrichment in KC 102 #1. The duration of erosion or non-deposition at the top Cenomanian appears to lessen from KC 102 #1 to Norton. Baha II is in a more distal position along the EFT fan and shows possible Turonian-Coniacian erosion or non-deposition with Santonian organic-rich beds remaining in Baha II. The Norton well lies on the northwestern flank of the EFT or PW fans in a shallower more proximal position during the mid-Cretaceous ([Pindell and Kennan, 2007](#); [Snedden et al., 2016](#)). Therefore, it may have experienced less post-Cenomanian erosion or non-deposition and less oxygen deficiency during OAE 3 as the paleogeographically deeper-water wells. The origin of the Cenomanian unconformity/disconformity observed here is beyond the scope of this paper.

### DISCUSSION

The observation that extensive deep-water siliciclastic deposition began as early as the Albian in the northern Gulf of Mexico has significant paleogeographic implications for the distribution of the updip fluvial systems that must have fed these submarine fans ([Fig. 9](#)). Detrital zircon provenance data published by [Blum and Pecha \(2014\)](#) suggests that most North American drainage systems were north flowing into the Boreal Sea with much smaller drainage systems coming out of the southern Appalachians and the modern day Gulf Coastal Plain feeding into the Gulf of Mexico.

Detrital zircon age data and sediment volume estimates by [Snedden et al. \(2022\)](#) illustrate the increase in siliciclastic sediment flux to the northern Gulf of Mexico that began in the earlier Albian and reached a maximum in the Cenomanian to Coniacian stages of the EFT supersequence ([Fig. 9](#)). Available detrital zircon data combined with well log subsurface mapping suggest a shift in provenance from the paleo-Apalachicola to the paleo-Mississippi depocenters (and associated paleo-rivers) during this time ([Fig. 9](#)). Occurrence of these thick, relatively coarse-grained, deep-water deposits suggests an elevated influx of siliciclastic sediment to prograde deltas across the older Albian carbonate shelf during this Greenhouse time of relatively high global sea level. We infer the presence of shelf-edge canyons or directly fed slope channels that acted as conduits routing sediment, especially sand, to the fans encountered at the KC 102 #1 well. Studies of modern day continental margins indicate that large volumes of sand can not move across wide continental shelves ([Sweet and Blum, 2016](#)). Without detrital zircon data from the KC 102 #1 well, it is impossible to say with certainty whether the deep-water sandstones seen in the well came primarily from a paleo-Apalachicola, or paleo-Mississippi source.

Depth (ft) White Light Fluorescent Light

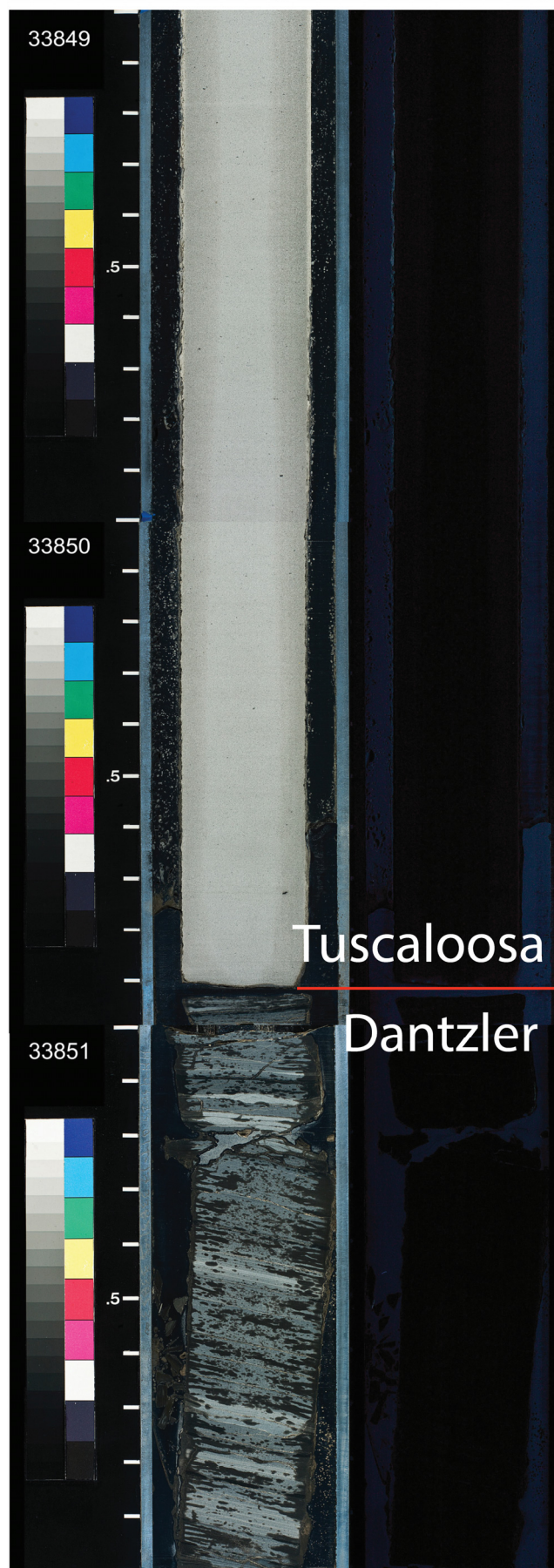


**Figure 6. Core photo showing the contact at the base of the Cenomanian Tuscaloosa Group where it rests unconformably on Albian mudstones.**

Although the results of the KC 102 #1 well demonstrate the presence of sand-rich submarine fans in the area, log and KC #1 core data show that these sandstones are highly quartz cemented and have low porosity and permeability (Sweet et al., 2021). In the KC area, the Cretaceous section lies below a very thick Paleogene section. As a result, exploration has shifted east to the MC area where the Paleogene is much thinner and the Cretaceous section is less deeply buried. It remains to be seen if the two wells drilled in this area, Galapagos Deep and Silverbank, have encountered thick Cretaceous sandstones with sufficient rock properties to be effective reservoirs.

The distribution of organically enriched sediments suggests that rather than being related to a single OAE the organic-rich beds in the Norton, Baha II, and KC 102 #1 wells were to be distributed between OAE's 1, 2, and 3. The hiatus associated with post-Cenomanian erosion or non-deposition separating OAEs 2 and 3 occurs later in time than the post-Albian abandonment of sand delivery to deep water occurring between deposition of the PW and EFT submarine fans. Although the origins of the OAEs are global in nature, regional and local paleo-environmental factors often modify the timing and quality of the resulting organic-rich rocks. Nutrient supply across shelves driven by eustatic rise and fluvial input has been recognized as key for enhancing marine productivity and oxygen deficiency during OAE 2 in the northern Gulf of Mexico (Lowery et al., 2017). The high mid-Cretaceous sediment flux spanning much of the Cenomanian to Coniacian stages (Snedden et al., 2022) indicates the northern Gulf of Mexico river systems may have also contributed a high nutrient supply, strengthening OAEs 2 and 3 and organic enrichment in the sediments. Provided adequate thermal maturities are reached in kitchen areas, the thickness, quality, and close stratigraphic proximity of these OAE organic-rich beds and PW and EFT submarine fan sands reduces petroleum charge risk for this potential play. The region of recognized mixed or exclusively Cretaceous-sourced oils in the northern Gulf of Mexico extends along the outer shelf and upper slope from Ewing Bank to Mississippi Canyon (Ferworm et al., 2003; Weimer et al., 2017) (Fig. 5).

## CONCLUSIONS

Newly released data from the KC 102 #1 (Tiber) well shows the presence of thick, coarse-grained, deep-water deposits that range in age from Albian to Cenomanian. These deposits are up to 350 mi from the contemporaneous shelf edge. We interpret their siliciclastic source to the paleo-Apalachicola to the paleo-Mississippi rivers that drained the southern Appalachian Mountains at this time.

The presence of thick Cretaceous submarine fan deposits suggest a new deep-water play in the Gulf of Mexico is emerging. As organic-rich Cenomanian and Coniacian shales overlie these thick sandstones, sealing risk is reduced. These organic-rich sediments may also act as source rocks. In KC, these sandstones have low porosity and permeability due to deep burial by a thick Paleogene section. Two recent exploration wells have tested this play further east in the MC protraction area where the Paleogene is considerably thinner and the Cretaceous is not as deeply buried. Time will tell if this play will be successful. Most frontier deepwater plays begin with a series of dry holes that often yield critical information that sets up later discoveries.

## KC 102 #1 Albian Section

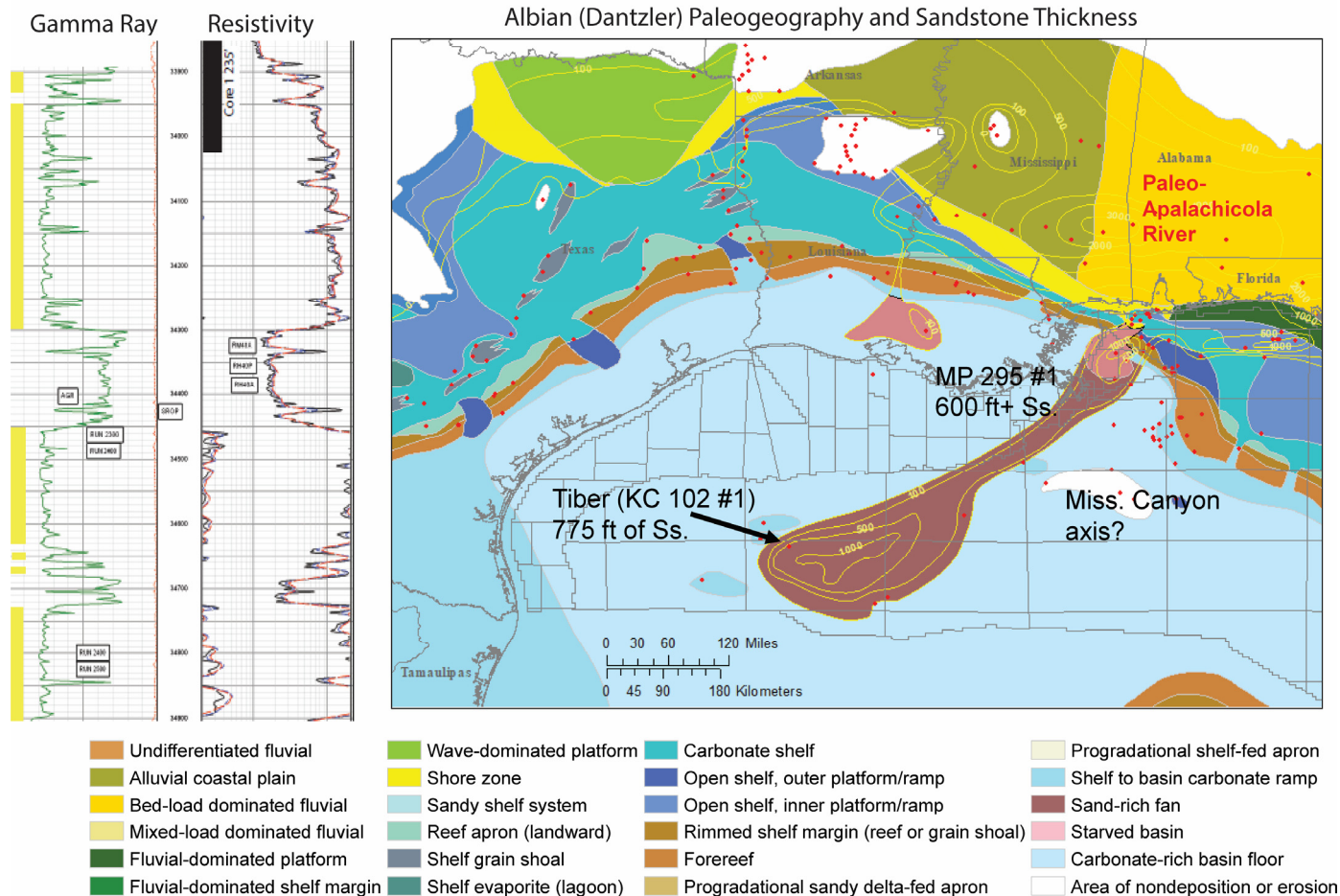


**Figure 7. Paleogeography at the time of the PW supersequence (Albian). Sandstones thickness contours in yellow. Section of the well logs from the KC 102 #1 well shows the thick deep-water sandstones deposited in this interval on submarine fans.**

### ACKNOWLEDGMENTS

We appreciate careful reviews by Amanda Mosola and Gillian Apps that helped us improve the quality of this paper. The Gulf Basin Depositional Synthesis Project (GBDS) Industrial Associates Program at The University of Texas at Austin Institute for Geophysics supported this research.

### REFERENCES CITED

Barrell, K. A., 1997, Sequence stratigraphy and structural traps styles of the Tuscaloosa trend: Gulf Coast Association of Geological Societies Transactions, v. 47, p. 27–34.

Bergen, J., 2009, BP Keathley Canyon 102–1 (Tiber prospect) nanofossil biostratigraphic summary, <<https://www.data.bsee.gov/>>.

Blum, M., and M. Pecha, 2014, Mid-Cretaceous to Paleocene North American drainage reorganization from detrital zircons: Geology, v. 42, p. 607–610, <<https://doi.org/10.1130/G35513.1>>.

Boulesteix, K., M. Poyatos-More, D.–M. Hodgson, S. S. Flint, and K. G. Taylor, 2020, Fringe or background: Characterizing deep-water mudstones beyond the basin-floor fan sandstone pinchout: Journal of Sedimentary Research, v. 90, p. 1678–1705, <<https://doi.org/10.2110/jsr.2020.048>>.

Corbett, M. J., D. K. Watkins, and J. J. Popspichal, 2014, A quantitative analysis of calcareous nanofossil bioevents of the Late Cretaceous (late Cenomanian–Coniacian) Western Interior Seaway and their reliability in established zonation schemes: Marine Micropaleontology, v. 109, p. 30–45, <<https://doi.org/10.1016/j.marmicro.2014.04.002>>.

Ferrow, K., J. Zumberge, and S. Brown, 2003, Integration of geochemistry and reservoir fluid properties: Bureau of Economic Geology, Petroleum Technology Transfer Council (PTTC) Workshop—First Annual Fluids Symposium on Reservoir Fluids 2003–PVT and Beyond, 51 p.

Houghton, P., C. Davis, W. McCaffrey, and S. Barker, 2009, Hybrid sediment gravity flow deposit—Classification, origin, and significance: Marine and Petroleum Geology, v. 26, p. 1900–1918, <<https://doi.org/10.1016/j.marpetgeo.2009.02.012>>.

Locklair, R., B. Sageman, A. and Lerman, 2011, Marine carbon burial flux and the carbon isotope record of Late Cretaceous (Coniacian–Santonian) Oceanic Anoxic Event III: Sedimentary Geology, v. 235, p. 38–49, <<https://doi.org/10.1016/j.sedgeo.2010.06.026>>.

Lowery, C. M., R. Cunningham, C. D. Barrie, T. Bralower, and J. W. Snedden, 2017, The northern Gulf of Mexico during OAE2 and the relationship between water depth and black shale development: Paleoclimatology, v. 32, p. 1316–1335, <<https://doi.org/10.1002/2017PA003180>>.

Lowe, D., 1982, Sediment gravity flows II: Depositional models with special reference to the deposits of high-density turbidity currents: Journal of Sedimentary Research, v. 52, p. 279–297, <<https://doi.org/10.1306/212F7F31-2B24-11D7-8648000102C1865D>>.

Lu, Y., R. D. Weber, R. V. Roederer, T. M. Reilly, J. A. Edmunds, N. R. Myers, and A. J. Avery, 2019, Biostratigraphic chart—

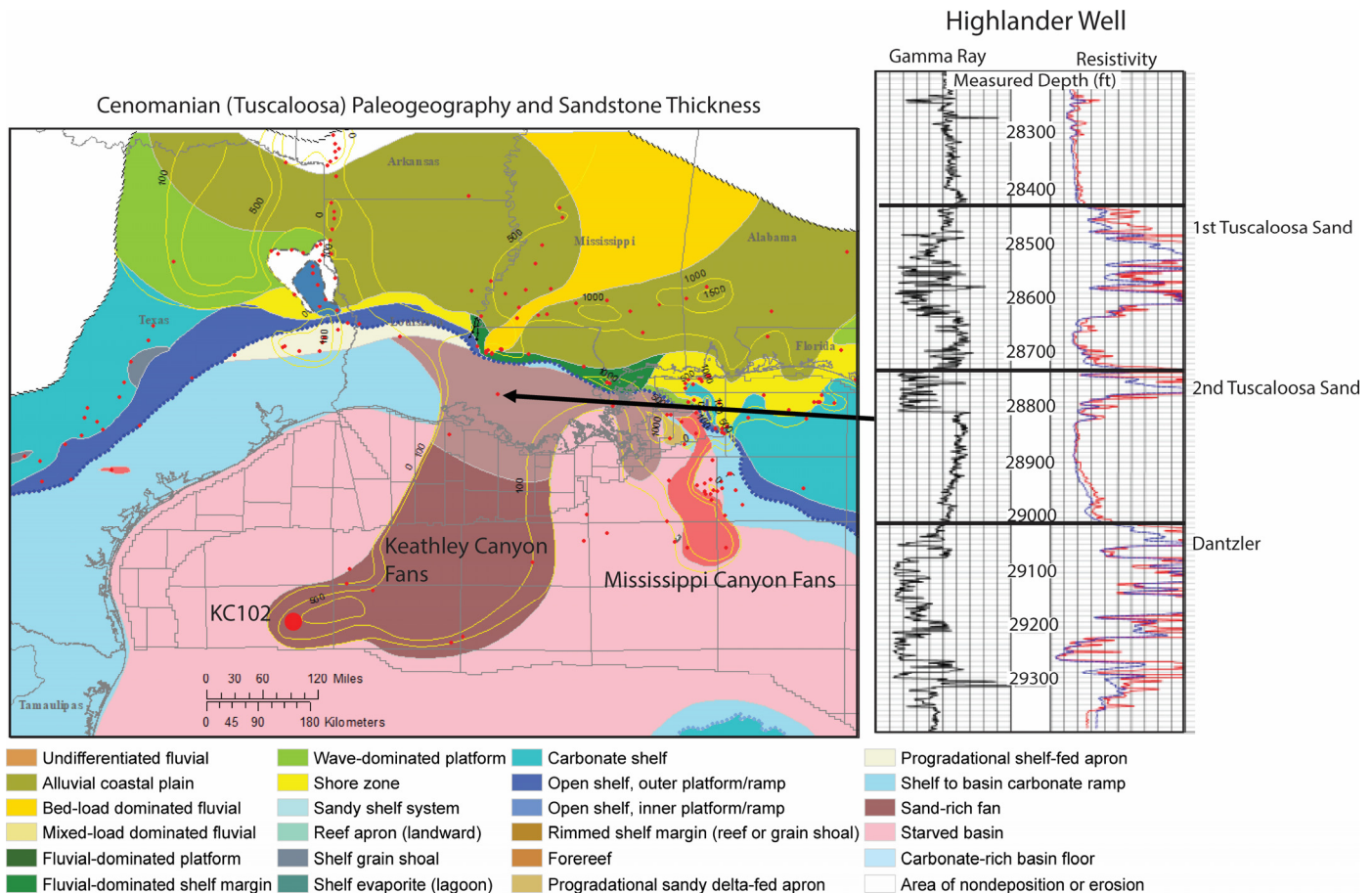


**Figure 8. Paleogeography at the time of the EFT supersequence (Cenomanian-Turonian). Sandstones thickness contours in yellow. Section of the well logs from the Highlander well shows the thick sandstones interpreted as slope-channel-filled deposits that were part of the system routing sand to submarine fans in Keathley Canyon.**

- Gulf Basin, USA: Cretaceous and Late Jurassic, <<https://www.paleodata.com/chart/>>.
- Mancini, E. A., R. M. Mink, B. L. Bearden, and R. P. Wilkerson, 1985, Norphlet Formation (Upper Jurassic) of southwestern and offshore Alabama: Environments of deposition and petroleum geology: American Association of Petroleum Geologists Bulletin, v. 69, p. 881–898, <<https://doi.org/10.1306/AD462B14-16F7-11D7-8645000102C1865D>>.
- Marchand, A. M. E., G. Apps, W. Li, and J. R. Rotzien, 2015, Depositional processes and impact on reservoir quality in deepwater Paleogene reservoirs, US Gulf of Mexico: American Association of Petroleum Geologists Bulletin, v. 99, p. 1635–1648, <<https://doi.org/10.1306/04091514189>>.
- Ogg, J., G. Ogg, and F. Gradstein, 2016, A concise geologic time scale 2016: Elsevier Science & Technology, U.K., 240 p.
- Perch-Nielsen, K., 1985, Cenozoic calcareous nannofossils, in H. M. Bolli, J. B. Saunders, and K. Perch-Nielsen, eds., Plankton stratigraphy: Cambridge University Press, U.K., p. 427–554.
- Phelps, R. M., C. Kerans, R. G. Loucks, R. O. B. P. Da Gama, J. Jeremiah, and D. Hull, 2014, Oceanographic and eustatic control of carbonate platform evolution and sequence stratigraphy on the Cretaceous (Valanginian-Campanian) passive margin, northern Gulf of Mexico: Sedimentology, v. 61, p. 461–496, <<https://doi.org/10.1111/sed.12062>>.
- Salvador, A., 1991, Origin and development of the Gulf of Mexico Basin, in A. Salvador, ed., The geology of North America, v. J: The Gulf of Mexico Basin: Geological Society of America, Boulder, Colorado, p. 389–444, <<https://doi.org/10.1130/DNAG-GNA-J.389>>.
- Sanford, J. C., J. W. Snedden, and S. P. S. Gulick, 2016, The Cretaceous-Paleogene boundary deposit in the Gulf of Mexico: Large-scale oceanic basin response to the Chicxulub impact: Geophysical Research: Solid Earth, v. 121, p. 1240–1261, <<https://doi.org/10.1002/2015JB012615>>.
- Snedden, J. W., J. Virdell, T. L. Whiteaker, and P. Ganey-Curry, 2016, A basin-scale perspective on Cenomanian-Turonian (Cretaceous) depositional systems, greater Gulf of Mexico (USA): Interpretation, v. 4, no. 1, p. SC1–SC22, <<https://doi.org/10.1190/INT-2015-0082.1>>.
- Snedden, J. W. and W. E. Galloway, 2019, The Gulf of Mexico sedimentary basin: Depositional evolution and petroleum applications: Cambridge University Press, U.K., 344 p., <<https://doi.org/10.1017/978110829279>>.
- Snedden, J. W., R. C. Cunningham, and Virdell, 2020, The northern Gulf of Mexico offshore super basin: Reservoirs, source rocks, seals, traps, and successes: American Association of Petroleum Geologists Bulletin, v. 104, p. 2603–2642, <<https://doi.org/10.1306/09092020054>>.
- Snedden, J. W., H. L. Hull, T. L. Whiteaker, J. W. Virdell, and C. H. Ross, 2022, Late Mesozoic sandstone volumes recorded in Gulf of Mexico subsurface depocentres: Deciphering long-term sediment supply trends and contributions by paleo river systems: Basin Research, v. 34, p. 1269–1291, <<https://doi.org/10.1111/bre.12659>>.
- Swanson, S. M., C. B. Enomoto, K. O. Dennen, B. J. Valentine, and C. D. Lohr, 2013, Geologic model for the assessment of undiscovered hydrocarbons in the Lower and Upper Cretaceous carbonate rocks of the Fredericksburg and Washita groups: US

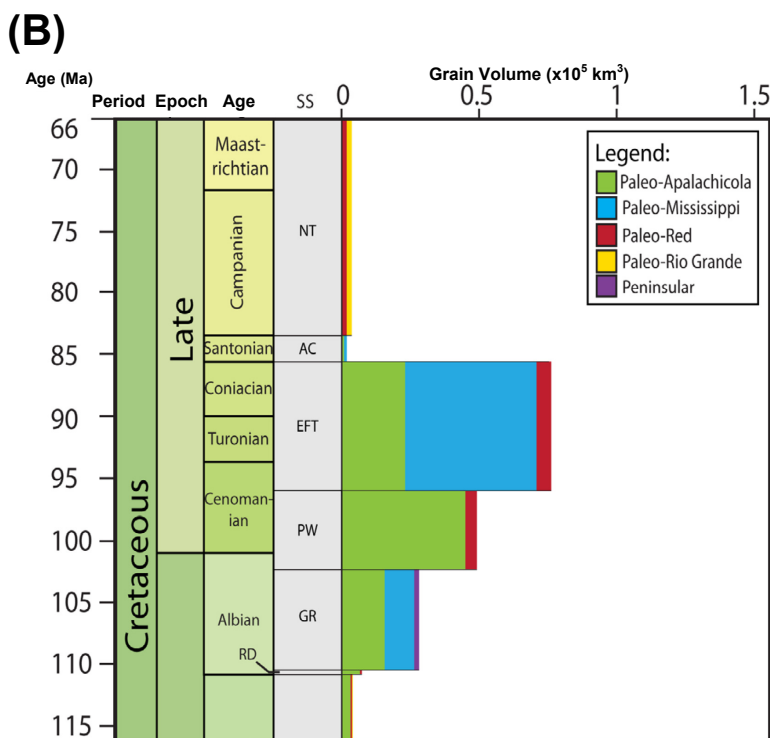
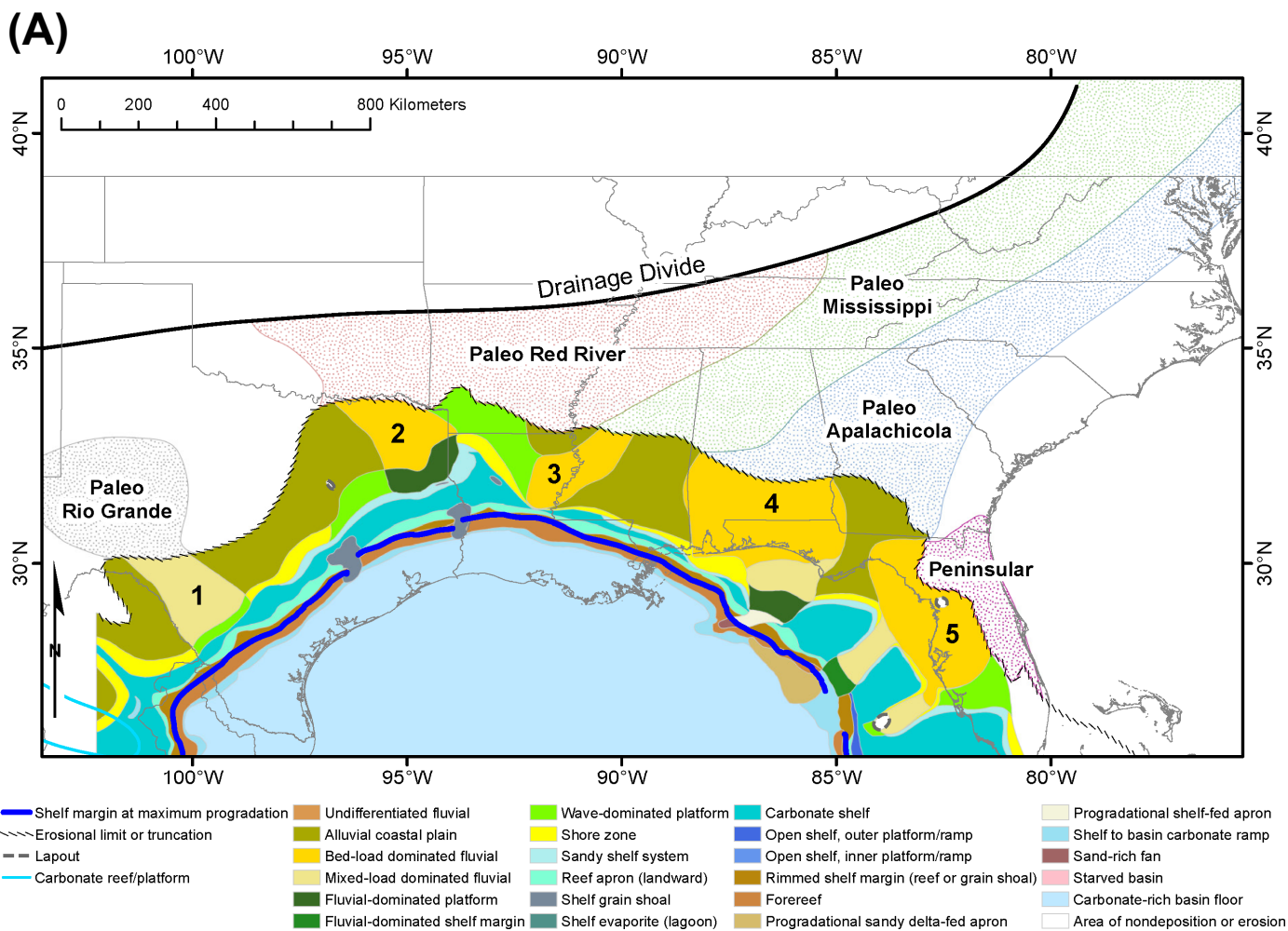


Figure 9. (A) Mesozoic drainage systems and depocenters of the northern Gulf of Mexico (from [Snedden et al. \[2022, their figure 2\]](#)). (B) Cretaceous sediment volumes for the northern Gulf of Mexico (from . Drainage systems (e.g., paleo-Apalachicola) derived from detrital zircon data (modified after [Snedden et al. \[2022, their figure 8\]](#)).

- Gulf Coast region: Gulf Coast Association of Geologic Societies Transactions, v. 63, p. 423–437.
- Sweet, M. L., and M. D. Blum, 2016, Connection between fluvial to shallow marine environments and submarine canyons: Implications for sediment transfer to deep water: Journal of Sedimentary Research, v. 86, p. 1147–1162, <<https://doi.org/10.2110/jsr.2016.64>>.
- Sweet, M. L., J. W. Snedden, M. Purkey, and R. Weber, 2021, Tiber Deep (Keathley Canyon 102): New insights into Upper Cretaceous deepwater plays in the northern Gulf of Mexico, part 1: Lithofacies and reservoir quality trends: GeoGulf Transactions, v. 71, p. 289–297.
- Waterman, A. S., R. D. Weber, Y. Lu, R. A. George, T. M. Reilly, R. V. Roederer, J. A. Edmunds, B. W. Parker, N. R. Myers, and A. J. Avery, 2017, Biostratigraphic chart—Gulf Basin, USA: Paleogene, <<https://www.paleodata.com/chart/>>.
- Weimer, P., R. Bouroullec, J. Adson, and S. P. Cossey, 2017, An overview of the petroleum systems of the northern deep-water Gulf of Mexico: American Association of Petroleum Geologists Bulletin, v. 101, p. 941–993, <<https://doi.org/10.1306/09011608136>>.
- Woolf, K. S., 2012, Regional character of the lower Tuscaloosa formation depositional systems and trends in reservoir quality: Ph.D. Dissertation, University of Texas at Austin, 226 p.

## APPENDIX

This Appendix includes a plate that is provided in the digital version of this paper. [Digital Plate 1](#) provides a biostratigraphic interpretation for the KC 102 #1 well.

### Tiber Calcareous Nannofossils

*Rhagodiscus angustus*  
*Cribrosphaerella ehrenbergii*  
*Micula decussata*  
*Micula concava*  
*Eiffelithus turriseiffelii*  
*Eiffelithus eximius*  
*Zeugrhabdotus embergeri*  
*Tranolithus orionatus*  
*Corollithion kennedyi*  
*Nannoconus regularis*  
*Rhagodiscus achlyostaurion*  
*Eprolithus floralis*  
*Rhagodiscus asper*  
*Broinsonia signata*  
*Rhagodiscus splendens*  
*Chiastozygus platyrhetus*  
*Axopodorhabdus albanius (biramiculatus)*  
*Prediscosphaera columnata*  
*Braarudosphaera stenorhetha*  
*Nannoconus truitii*

### Tiber Foraminifera

*Hedbergella planispira*  
*Clavihedbergella simplex*  
*Praeglobotruncana delrioensis*  
*Rotalipora gandolfi*  
*Rotalipora appenninica*  
*Muricohedbergella (Hedbergella) delrioensis*  
*Rotalipora subticinensis*  
*Ticinella roberti*  
*Rotalipora spp.*

API: 608084001500  
 AREA: Keathley Canyon  
 BLOCK: 102  
 OCS (Lease): 25782  
 WELL NUMBER: 1  
 OPERATOR: BP  
 PALEONTOLOGIST: Jim Bergen (original, 2009); Marcie P. Phillips (re-interpretation, 2022)  
 SAMPLES: 25110-35000 ft

# Tiber KC 102 #1 Biostratigraphic Interpretation

